Supplementary Material for:

Stepped spin crossover in Fe(III) halogen substituted quinolylsalicylaldimine complexes

Wasinee Phonsri,[a,b] David J. Harding,*[a] Phimphaka Harding,[a]
Keith S. Murray,[b] Boujemaa Mourabaki,[b] Ian A. Gass,[b,c] John D. Cashion,[d]
Guy N. L. Jameson[e] and Harry Adams[f]

[a] Molecular Technology Research Unit, Walailak University, Thasala, Nakhon Si Thammarat, 80161, Thailand

[b] School of Chemistry, Monash University, Clayton, Melbourne, Victoria, 3800, Australia

[c] Now at the School of Pharmacy and Biomolecular Sciences, University of Brighton, Brighton, BN2 4GJ, UK

[d] School of Physics, Monash University, Melbourne, Victoria, 3800, Australia

[e] Department of Chemistry & MacDiarmid Institute for Advanced Materials and Nanotechnology, University of Otago, P.O. Box 56, Dunedin 9054, New Zealand

[f] Department of Chemistry, University of Sheffield, Sheffield, S3 7HF, UK

* Corresponding author. E-mail: hdavid@wu.ac.th

SQUID Magnetometry

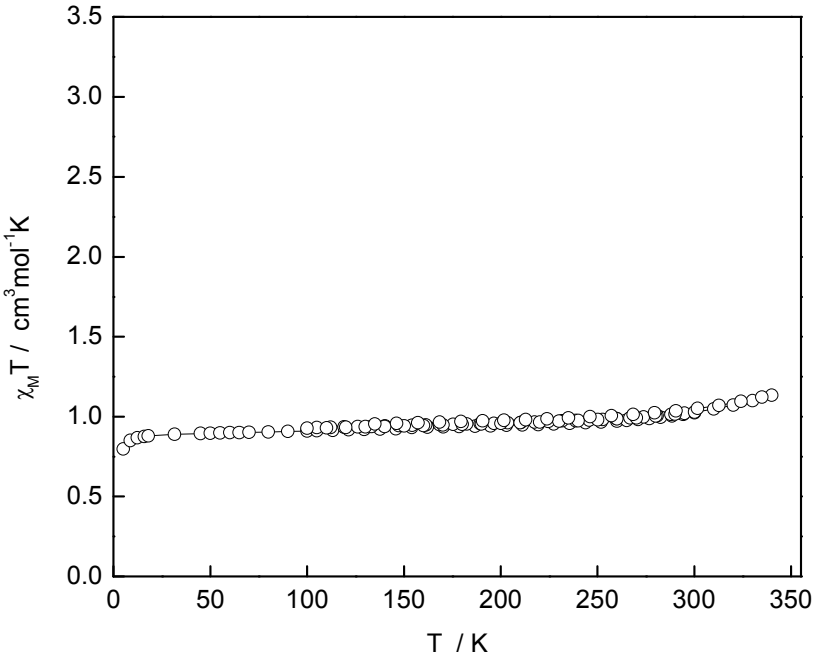

Figure S1 Thermal variation of $\chi_M T$ versus T plot for $[Fe(qsal\text{-}I)_2]NCS \cdot 0.25CH_2Cl_2 \cdot 0.5MeOH$ **4**.

^{1}H NMR and UV-Vis Spectroscopic Solution Studies

The ^{1}H NMR studies to determine the magnetic susceptibility of [Fe(qsal-X)$_2$]NCS were recorded at 298 K in d^6-DMSO with TMS added as an internal standard against a reference of d^6-DMSO with TMS added on a 300 MHz Bruker FT-NMR spectrometer following a modified Evan's method. The reference solvent was placed in a co-axial insert with the solution of the complex in a standard NMR tube. The mass susceptibility was calculated using:

$$\chi_g = \chi_o + \frac{3\Delta v}{4\pi v_o c}$$

where χ_o = the mass susceptibility of DMSO (-0.629 x 10^{-6} $cm^3 \cdot g^{-1}$), $\Delta\upsilon$ (Hz) is the paramagnetic shift of the reference, υ_o is the operating RF frequency of the NMR spectrometer (300.13 x 10^6 Hz) and *c* is the concentration of the solution in $g \cdot cm^{-3}$. The mass susceptibility was then converted to molar susceptibility (χ_M). Diamagnetic corrections were applied and by multiplication with the measurement temperature (298 K) $\chi_M T$ was determined.

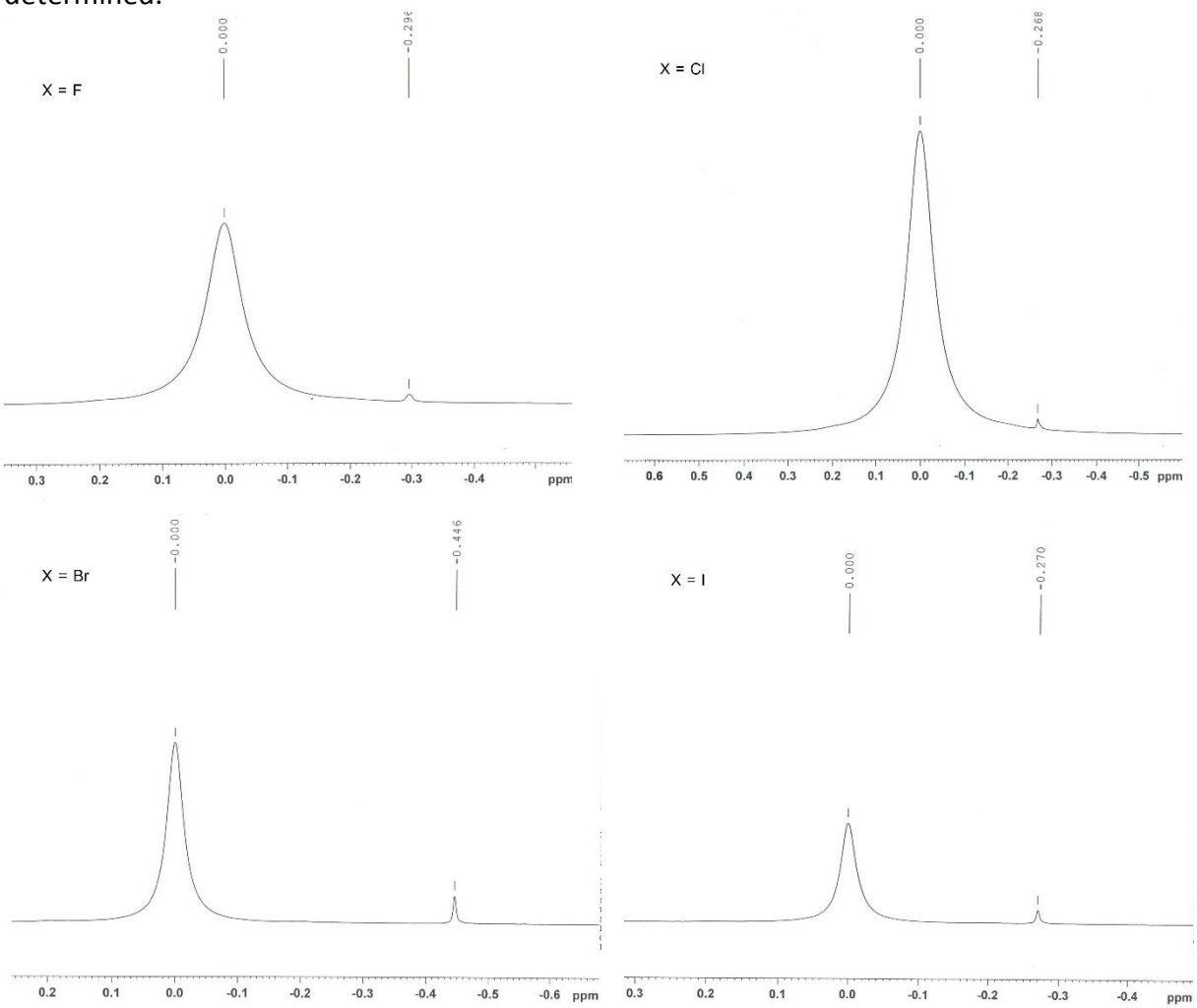

Figure S2 ^{1}H NMR spectrum of [Fe(qsal-X)$_2$]NCS in d^6-DMSO showing the TMS shift.

Table S1 Selected ^{1}H NMR data of **1-4** in d^{6}-DMSO at 298 K.

Compound	Concentration (g/cm^{3})	Δυ (Hz)	χ_MT (cm^{3}·mol^{-1}·K)	%HS
[Fe(qsal-F)$_2$]NCS	0.0085	88.83	1.57	29
[Fe(qsal-Cl)$_2$]NCS	0.0100	80.43	1.27	22
[Fe(qsal-Br)$_2$]NCS	0.0103	133.86	2.32	49
[Fe(qsal-I)$_2$]NCS	0.0093	81.04	1.73	34

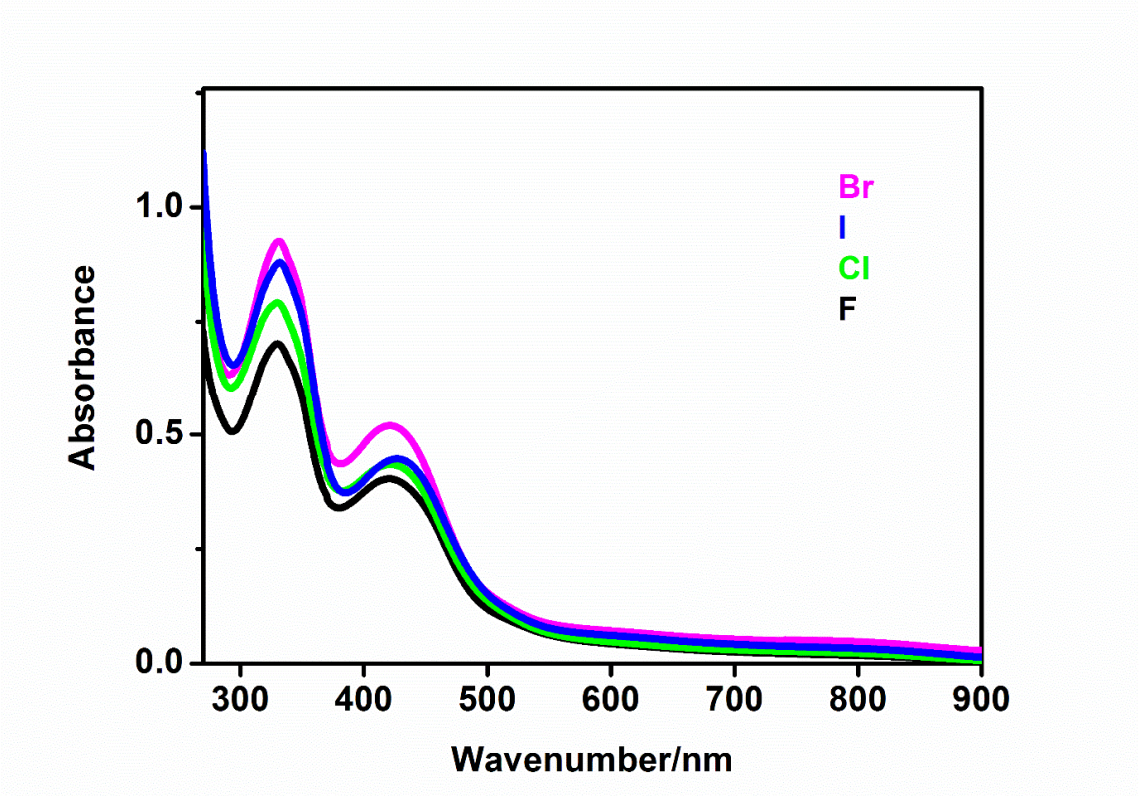

Figure S3 UV-Vis spectra of **1**-**4** in DMSO.

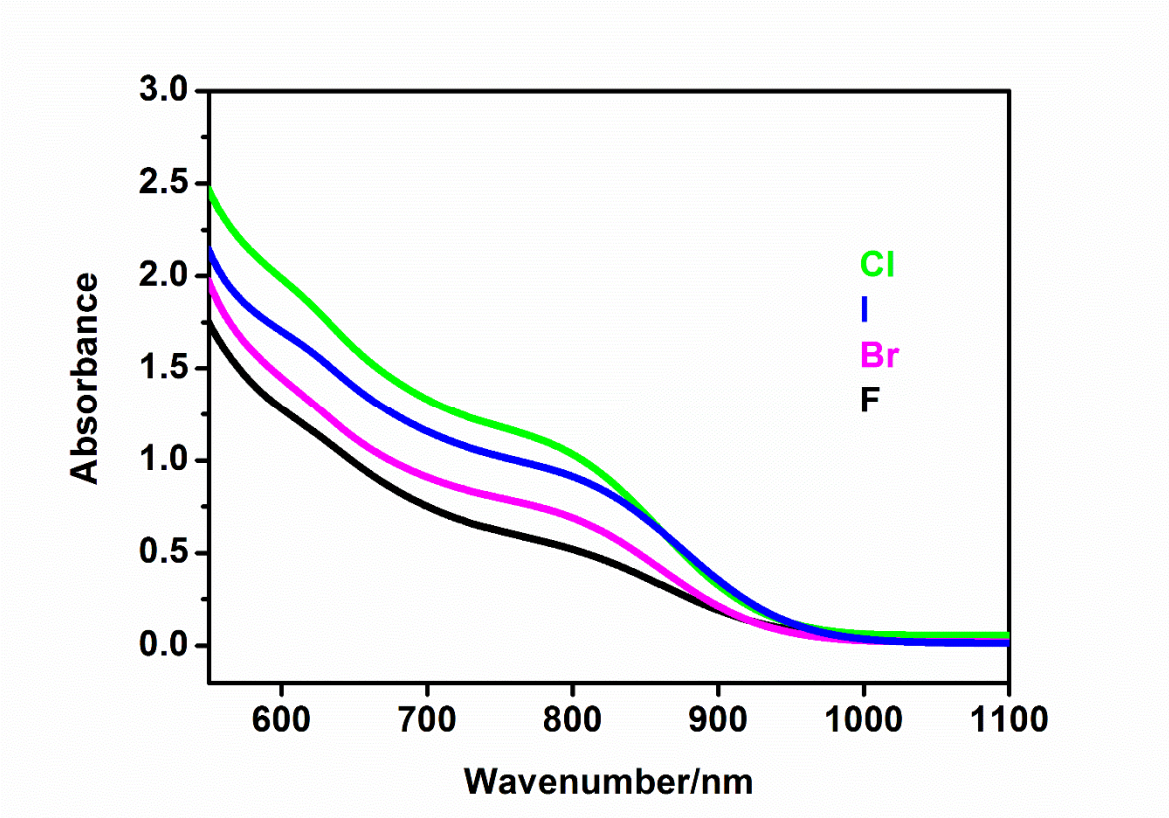

Figure S4 UV-Vis spectra of **1**-**4** in DMSO showing the shoulder at *ca*. 800 nm.

Thermal Analysis

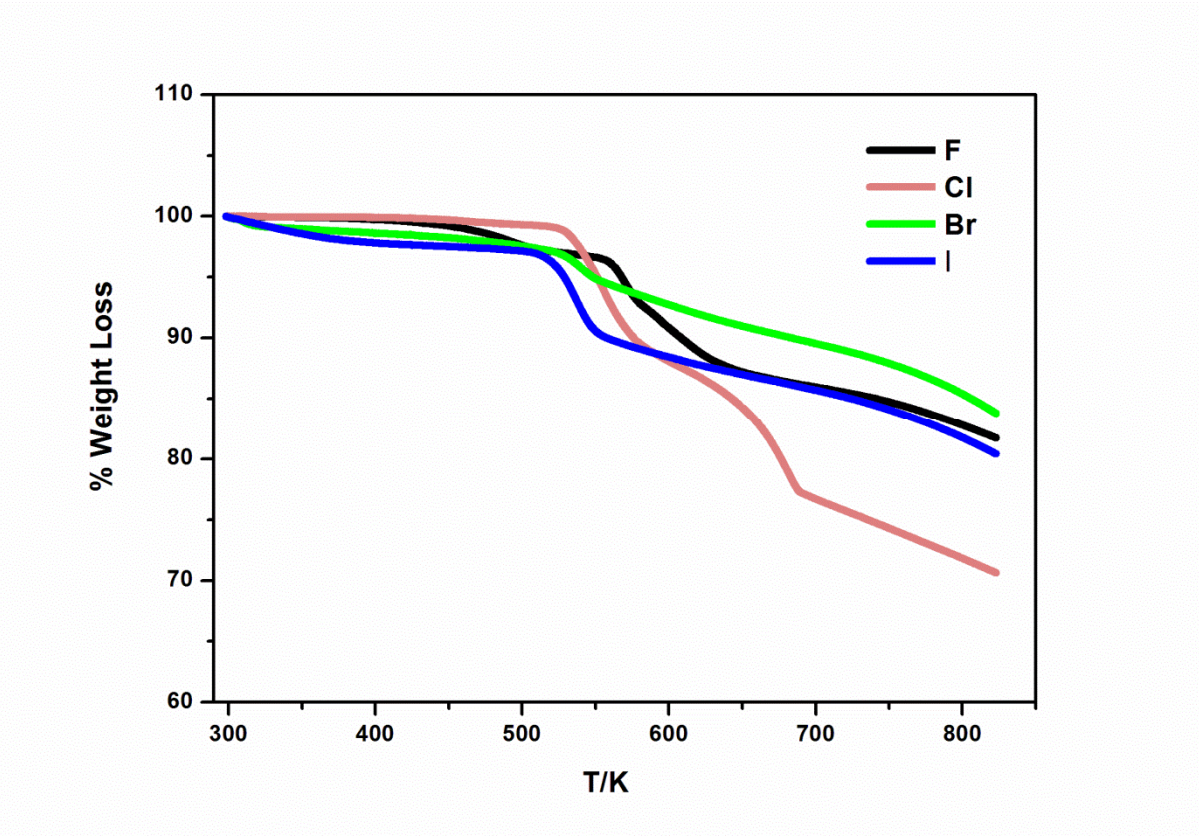

Figure S5 Thermogravimetric analysis of **1**-**4**.

X-ray Crystallographic Figures and Tables

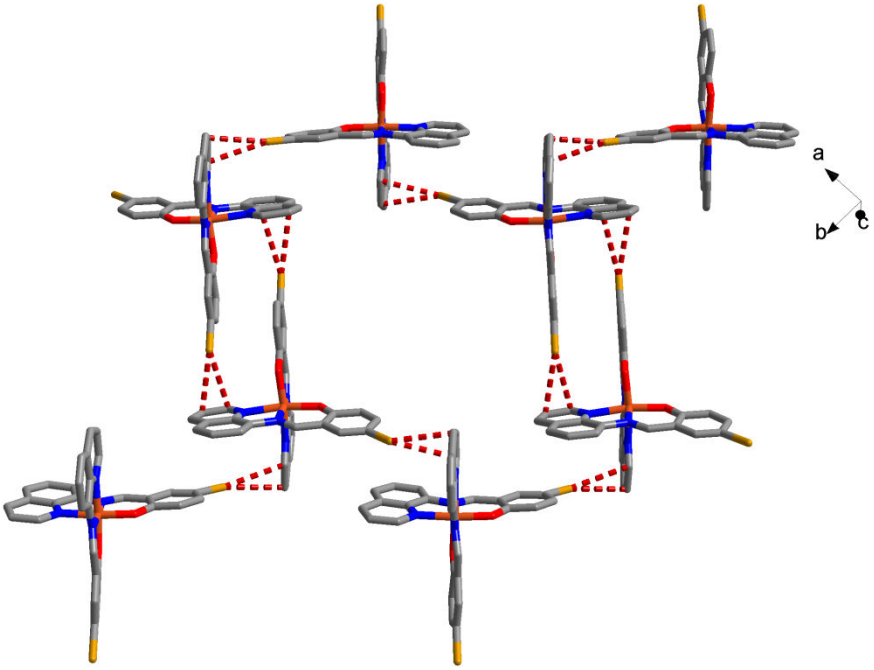

Figure S6 Br···π interactions that link the cations on the *ab* plane in $[Fe(qsal\text{-}Br)_2]NCS\cdot MeOH$ **3** at 123 K.

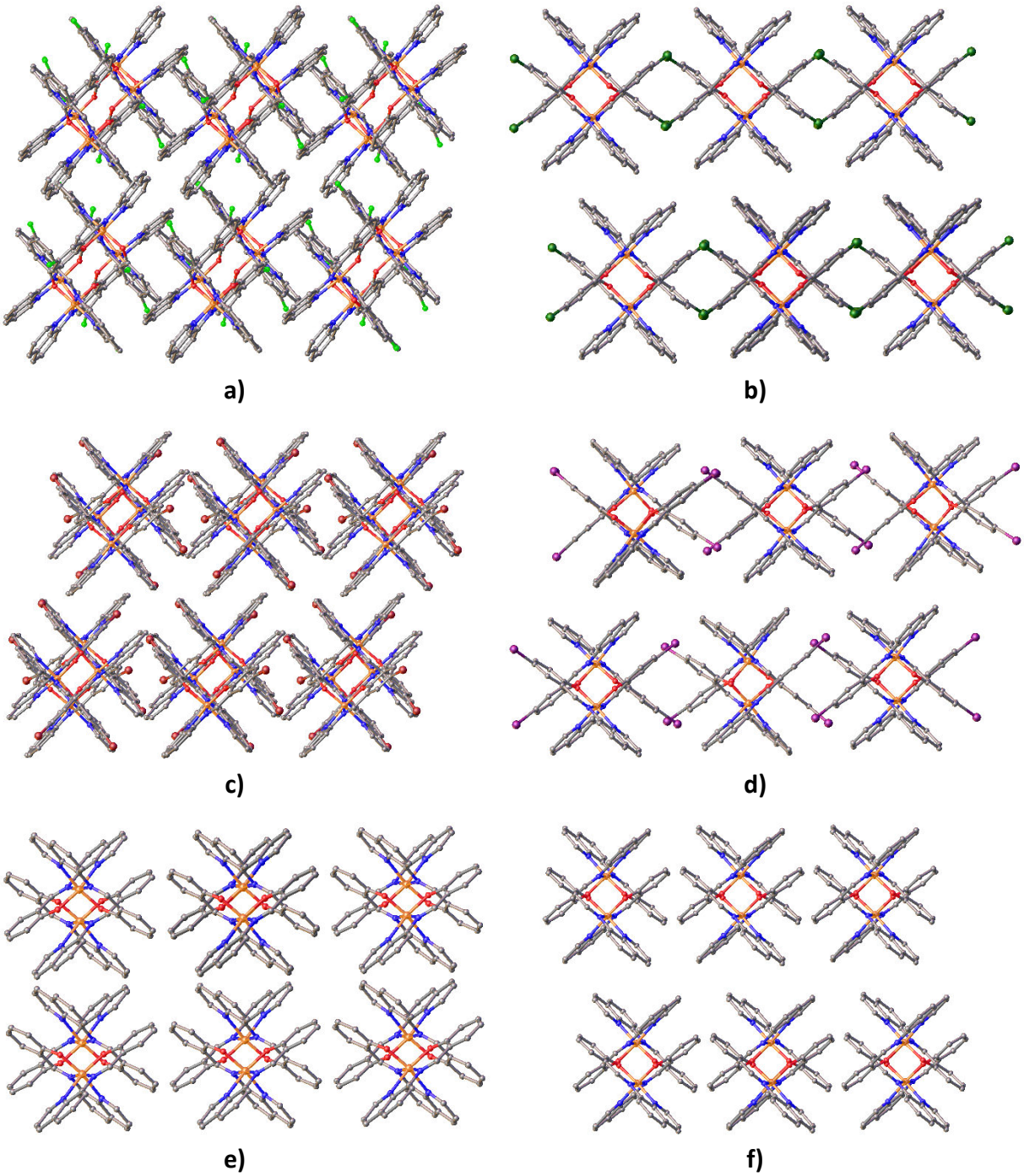

Figure S7 View of the overall packing in a) $[Fe(qsal\text{-}F)_2]NCS$ (123 K), b) $[Fe(qsal\text{-}Cl)_2]NCS\cdot MeOH$, c) $[Fe(qsal\text{-}Br)_2]NCS\cdot MeOH$ (123 K), d) $[Fe(qsal\text{-}I)_2]NCS\cdot 0.25CH_2Cl_2\cdot 0.5MeOH$ e) $[Fe(qsal)_2]NCS$ (**HS**) and f) $Fe(qsal)_2]NCS\cdot CH_2Cl_2$ (**LS**) viewed down the 1D π-π chains.

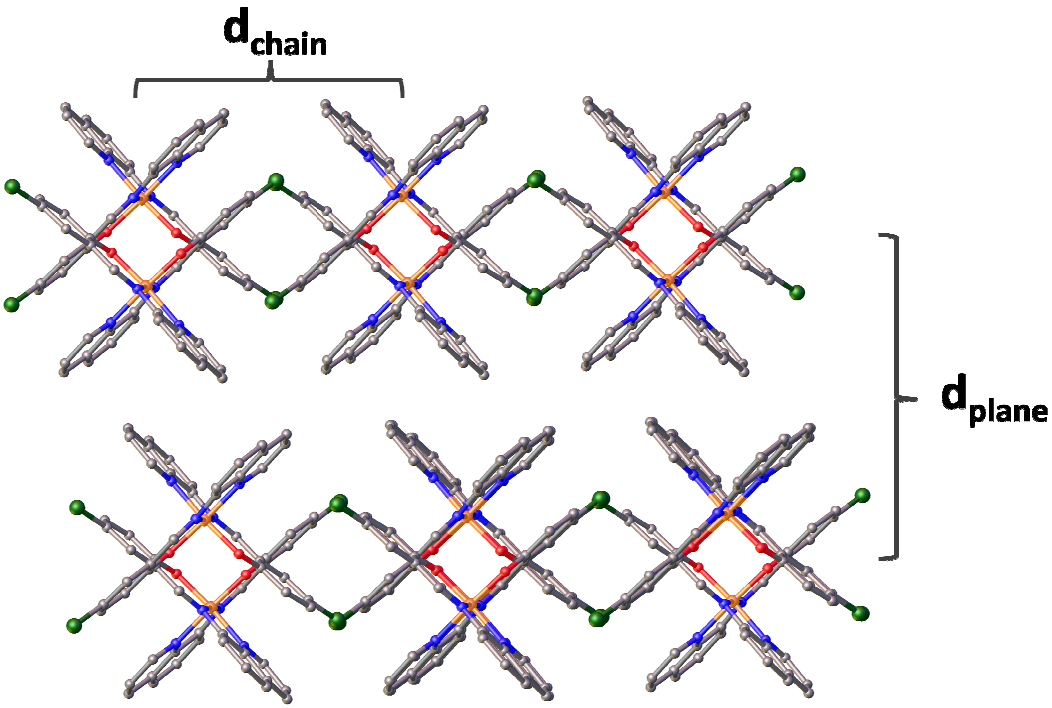

Figure S8 Representation of the d_{chain} and d_{plane} distances in [Fe(qsal-X)$_2$]NCS structures.

Table S2 Interchain (d_{chain}) and Interplanar (d_{plane}) distances in **1**-**4**.

Compound	**d_{chain} (Å)**[a]	**d_{plane} (Å)**[a]
[Fe(qsal-F)$_2$]NCS	9.87	12.00
[Fe(qsal-Cl)$_2$]NCS·MeOH	10.02	12.10
[Fe(qsal-Br)$_2$]NCS·MeOH	10.18	12.78
[Fe(qsal-I)$_2$]NCS·0.25CH_2Cl_2·0.5MeOH	10.41	12.00
[Fe(qsal)$_2$]NCS[b]	9.69	12.50

[a] Calculated for the low temperature (LS) structure in each case except [Fe(qsal)$_2$]NCS for which only the HS structure is known.
[b] Calculated from *Chem. Eur. J.*, 2009, **15**, 3497–3508.

Table S3 Intermolecular interactions in [Fe(qsal-F)$_2$]NCS (Å).

Interactions	100 K	200 K	270 K
1D Chains			
π-π Type A (Fe1-Fe1)	3.234	3.226	3.253
Fe1···Fe1	7.265	7.424	7.434
π-π Type B (Fe2-Fe2)	3.315	3.520	3.525
Fe2···Fe2	7.390	7.371	7.340
O4···H41	2.715(2)	2.655(2)	2.703(2)
Fe1-Fe2 interactions			
O3···H5	2.550(2)	2.583(2)	2.631(2)
O2···H57	-	2.682(2)	-
F1···H42	2.550(2)	2.517(2)	2.502(2)
Fe1···Fe2	7.350	7.349	7.375
2D and 3D interactions			
F2···H58	2.492(2)	2.430(2)	2.465(2)
F4···H26	2.548(2)	2.420(2)	2.447(3)
F3···H9	-	2.511(2)	2.574(3)
F2···π	3.143	3.220	3.265
π-π	3.538	3.608	3.625
F3···π	3.133	3.101	3.124
π-π	3.611	3.544	3.593
NCS interactions			
S1···H31	2.566(1)	2.732(1)	2.774(1)
S1···H34	2.850(1)	-	-
S1···H51	2.818(1)	-	2.890(2)
S1···H61	2.770(1)	2.847(1)	2.857(2)
N9···H45	2.732(2)	2.639(4)	2.679(5)
N9···H63	2.518(2)	2.497(3)	2.578(5)
N9···H35	-	2.653(4)	-
N9···H43	-	2.687(4)	-

Table S4 Intermolecular interactions in $[Fe(qsal\text{-}Cl)_2]NCS\cdot MeOH$ (Å).

Interactions	100 K
1D chains	
π-π Type A	3.288
Fe1···Fe1 (Type A)	6.878
π-π Type B	3.350
Fe1···Fe1 (Type B)	6.980
C26-H26····O1	2.564(3)
C28-H28····O1	2.636(4)
C12-H12····O2	2.472(4)
Cl···π interactions	
Cl1····π (C_g = C17-C18)	3.238
Cl2····π (C_g = C1-C2)	3.286
P4AE	
C3-H3····π	3.298
π-π	3.632
NCS & MeOH interactions	
N5····H14-C14	2.533(6)
N5····H21-C21	2.711(6)
N5····H30-C30	2.533(6)
N5····H1S-O1S	2.016(8)
S1····H2-C2	2.924(2)
S1····H17-C17	2.803(2)
S1····H19-C19	2.951(2)
S1····C7	3.280(6)
C1S····H1	2.826(1)

Table S5 Intermolecular interactions in $[Fe(qsal\text{-}Br)_2]NCS\cdot MeOH$ (Å).

Interactions	**123 K**	**295 K**
1D chains		
π-π Type A (Fe1-Fe1)	3.125	3.180
Fe1···Fe1	6.918	6.967
O2···H7	2.582(4)	2.654(3)
π···Br1	3.476(7)	3.533(7)
π-π Type B (Fe2-Fe2)	3.319	3.403
Fe2···Fe2	6.831	6.861
O4···H53	2.531(5)	2.601(4)
Br3···H10 (Fe1-Fe2)	2.959(8)	3.017(8)
Fe1···Fe2	7.542	7.540
Br···π and C-H···Br interactions		
Br2···π (C_g = C62-C63)	3.304	3.351
Br3··· π	3.556(8)	3.596(9)
Br4···π	3.452(7)	3.588(8)
Br4···H26	2.976(7)	-
NCS & MeOH interations		
S1···H15	2.819(2)	2.886(2)
S1···H58	2.941(2)	3.016(2)
S1···C23	3.361(6)	3.405(5)
N9···H51	2.695(6)	2.774(9)
S2···H63	2.736(2)	2.807(3)
C68···H2	2.851(7)	2.992(2)
O6··· C55	3.183(9)	3.255(1)
O6···H47	2.533(5)	2.787(9)
S2···H29	2.725(3)	2.735(3)
N10···H19	2.541(7)	2.611(3)
S1···H45	2.767(2)	2.813(3)

Table S6 Intermolecular interactions in $[Fe(qsal\text{-}I)_2]NCS\cdot 0.25CH_2Cl_2\cdot 0.5MeOH$ (Å).

Interactions	**123 K**
<u>1D chains</u>	
π-π Type A (Fe1)	3.305
Fe1···Fe1	6.981
O1···H7-C7	2.622(4)
O2···H23-C23	2.711(4)
O2···H25-C25	2.680(4)
π-π Type B (Fe2)	3.399
Fe2···Fe2	6.992
O3···H39-C39	2.618(4)
I4···π	3.594(7)
<u>2D interactions</u>	
I4···H34-C34	3.082(4)

Mössbauer Spectroscopy

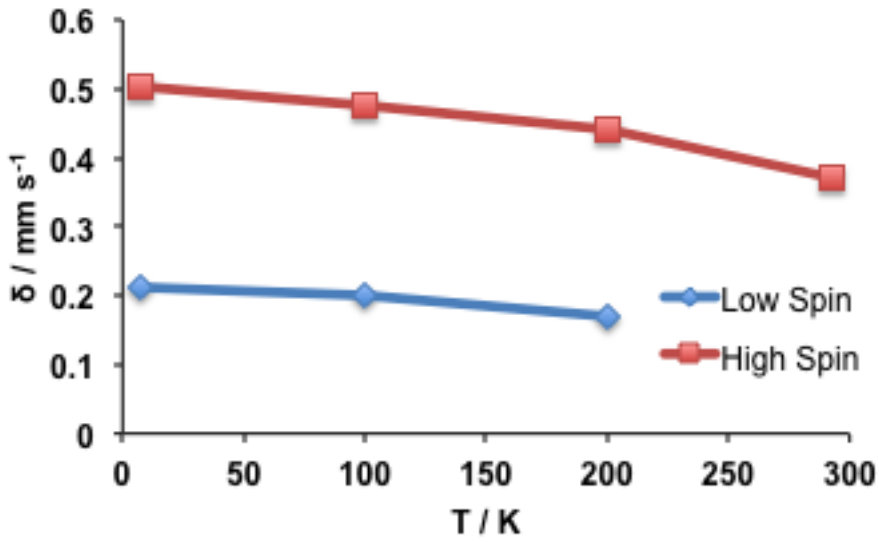

Figure S9 Decrease in isomer shift of both LS and HS **1** as the temperature is increased due to the second-order Doppler effect.

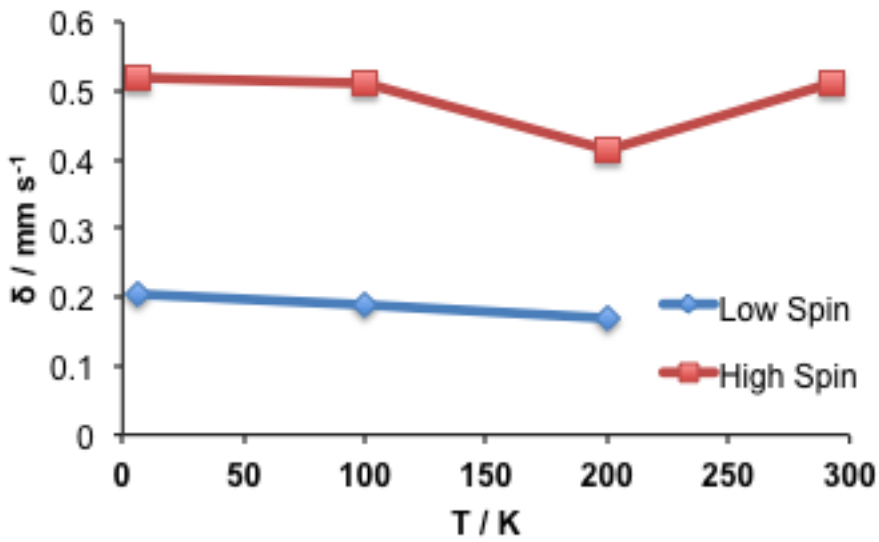

Figure S10 Temperature dependence of the isomer shift of both LS and HS **2** as the temperature is increased. Although there is a general decrease due to the second-order Doppler effect, the isomer shift of the HS species is seen to increase at higher temperatures indicating a possible structural change.